

Chapter 5 Mineral Chemistry of Crystalline Phases Within DSDP Leg 60 and ODP Leg 125 Ash Layers

5.1 Introduction

As discussed in Chapter 4 and Appendix 2, 64 representative ash layers from Site 458, and 71 layers from Site 459B were chosen from DSDP Leg 60; 22 representative ash layers from Site 782A, 16 layers from Site 784A, and 15 layers from Site 786A were selected from ODP Leg 125. These ash layers consist of glass and mineral shards, rock fragments and pelagic sediments (mostly nannofossil marls, clays, and chalks). Chapter 4 detailed the major element chemistry of glass shards. This Chapter will discuss nature of the mineral assemblages, mineral chemical composition, and inferred temperature and oxygen fugacity ($f\text{O}_2$) from the assumed coexisting two pyroxenes and Fe-Ti oxides.

The major element concentrations of the individual mineral shards from all these DSDP Leg 60 and ODP Leg 125 representative ash layers were determined by EMP-EDS. Approximately 2400 analyses of minerals (1034 for plagioclase, 867 for pyroxene, 477 for Fe-Ti oxides and a few for other minerals) were acquired from 186 bulk ash samples (133 DSDP Leg 60 ash layers and 53 ODP Leg 125 ash layers). All of these original data are given in Appendix 3.2. All the major and minor element data are normalised to 100 wt% volatile-free, with all Fe being reported as FeO^* except where otherwise indicated. The original total (wt%) values for each point analysis are also given in these tables. The ages assigned to the minerals are taken from the host ash layers (see Chapter 4 for explanation). ^{40}Ar - ^{39}Ar dating was attempted on some of the bulk ash layers with the help of Dr. M. Cosca (Universite de lausanne), but without success.

5.2 Mineral assemblages

Crystalline phases exist in almost every ash layer studied, occurring either mostly as discrete fragments or less commonly enclosed in glass. The latter case is particularly characteristic

with some of the plagioclase and clinopyroxene. Mineral sizes are generally larger than or similar to the glass shards except for Fe-Ti oxides, which are generally smaller than glass shards. The mineral shards are remarkably fresh throughout the sequences from Eocene to present in all five sites studied.

Plagioclase is the most common mineral and occurs in almost every ash layer. Pyroxene is also fairly common. In most cases, clinopyroxene is more abundant than orthopyroxene. The Fe-Ti oxide minerals include titanomagnetite, magnetite and ilmenite. Titanomagnetite is common but magnetite and ilmenite are relatively rare. Olivine is also rare occurring in 14 shards from DSDP Leg 60 Sites 458 and 459B at about 0.4-0.5 Ma, 2.6-2.8 Ma and 11.7 Ma (Table A 3-9). Other minerals such as garnet, amphibole, K-feldspar, titanite and apatite are found only in one to three shards. Three garnet shards were found in ashes from Sites 458 and 459B at 8.6 Ma, 18.8 Ma and 22.0 Ma (Table A 3-10), two amphibole fragments at Site 459B at 19.5 and 22.0 Ma (Table A 3-10), one K-feldspar and one titanite shard at Site 459B at 1.7 Ma, and one apatite at Site 459B at 35 Ma (Table A 3-11).

5.3 Mineral chemistry

Plagioclase is invariably zoned, usually in oscillatory fashion. The compositions of plagioclase from both DSDP Leg 60 sites and ODP Leg 125 sites are plotted in Figures 5-1 and 5-2. Clearly, the compositions of the two groups of plagioclase are very similar, and the most common range is from An₉₆ to An₅₀, regardless of the time intervals and Sites. The plagioclase is predominantly calcic with 18% anorthite (An₉₁₋₁₀₀), 52% bytownite (An₇₁₋₉₀), 25% labradorite (An₅₀₋₇₀) and less than 5% andesine (An₃₁₋₅₀). The composition of plagioclase from all ash layers sampled ranges from 43% to 58% SiO₂, 27% to 37% Al₂O₃, 9% to 20% CaO, 0.3% to 7% Na₂O and 0.08% to 0.4% K₂O. Interestingly, the plagioclase with higher K₂O contents (0.3-0.75%) coexist with the high-K glasses at ~ 2 Ma, ~ 8 Ma, ~ 22 Ma in DSDP Leg 60 Sites 458 and 459B, and high-K glasses at ~ 3 Ma and ~ 6 Ma in ODP Leg 125 Sites 782A and 784A (Figures 5-2 and 5-5).

The composition of pyroxene from both DSDP Leg 60 sites and ODP Leg 125 sites is shown in Figures 5-3, 5-4 and 5-5. Clinopyroxene, which is dominantly augite, is by far the most abundant of the mafic minerals. Minor pigeonite also occurs in two groups of ash layers. The compositional spread of pyroxene in ashes from the Izu-Bonin to Mariana arc, from Oligocene to present, is very similar (Figure 5-3). There is a boninitic (volcanic) basement beneath the lowermost ash layers at DSDP Leg 60 Site 458. Three of these ash layers were sampled. They contain Mg-rich orthopyroxene but no plagioclase, and the layers contain true boninitic glasses that are completely different from all other glass compositions sampled in the IBM region (see Chapter 9 for detailed discussion).

The composition of clinopyroxene (Cpx) from all ash layers sampled ranges from 49% to 54% SiO₂, 1% to 6% Al₂O₃, 0.2% to 0.7% TiO₂, 3% to 18% FeO*, 12% to 19% MgO, 0.2% to 0.8% MnO, 14% to 24% CaO, 0.15% to 0.5% Na₂O, and generally 0.65 to 0.95 Mg#* (Mg/(Mg+Fe*)), while the composition of all orthopyroxene (Opx) ranges from 49% to 54% SiO₂, 0.7% to 3.5% Al₂O₃, 0.15 % to 0.3% TiO₂, 16% to 33% FeO*, 18% to 30% (some lower to 13%) MgO, 0.4% to 1.8% MnO, 1% to 6% CaO, 0.2% to 0.4% Na₂O and 0.45 to 0.75 Mg#*. Compared with Cpx, Opx has lower Al₂O₃, TiO₂, Mg#* but higher FeO*, MgO, and MnO and very similar SiO₂ and Na₂O contents. The pyroxene from the near-basement boninitic ash layers is completely different from all other pyroxene in the ash layers, having the highest SiO₂ 55.5-57%, MgO 31-35% and Mg#* 0.85-0.90, lowest Al₂O₃ <1.5%, TiO₂ <0.15%, FeO* 6-10%, and MnO 0.15-0.4%. The Cr₂O₃ content in all pyroxene from all the ash layers studied is very low, most with < 0.13% and a minority with < 0.6%.

The compositions of the Fe-Ti oxides (titanomagnetite, magnetite and ilmenite) are listed in Appendix 3 and are plotted in Figures 5-6 and 5-7. The Fe-Ti oxides also exhibit a very similar compositional spread in ashes from DSDP Leg 60 Sites to ODP Leg 125 Sites and from Oligocene to present. The composition of titanomagnetites in all sampled ash layers ranges from 20% to 70% Fe₂O₃, 30% to 50% FeO, 5% to 24 % TiO₂, 0.5% to 5% Al₂O₃, 0.5% to 4% MgO, 0.2% to 2.2% MnO, 0.3% to 2% V₂O₃, and < 0.8% Cr₂O₃. There is no Fe-Ti oxide in the three lowermost boninitic ash layers. The composition of ilmenites ranges from 38% to 50% TiO₂, 40% to 54% FeO*, 0.1% to 0.8% Al₂O₃, 0.3% to 4.5% MgO, 0.4% to 2% MnO and < 0.13% Cr₂O₃.

The other minerals such as olivine, garnet, amphibole, K-feldspar, titanite and apatite are found only in one to fourteen shards in DSDP Leg 60 Sites 458 and 459B. Compositions of all these minerals are given in Appendix 3, Tables A 3-9 to 3-11. The olivine ranges from Fo₇₃₋₆₃ with one Fo₁₁ shard and one Fo₄₁ shard. It is possible that the K-feldspar is authigenic (Kastner, 1981).

5.4 Inferred temperature and oxygen fugacity

Ilmenite-titanomagnetite (Il-Mt) and Cpx-Opx pairs are found in many ash layers. All these data are listed in Appendix 3. No consistent temporal changes for these mineral compositions have been detected. In order to estimate the temperature and fO₂ ranges of the IBM arc system, the combined two-pyroxene thermometers of Wood and Banno (1973), Wells (1977), Lindsley (1983), and Brey and Kohler (1990), and single-pyroxene thermometer of Mercier (1976, 1980), and ilmenite-titanomagnetite thermometers of Buddington and Lindsley (1964), Stormer (1983) and Ghiorso and Sack (1991) are applied with the assumptions: 1) that the separate clinopyroxene and orthopyroxene, ilmenite and titanomagnetite crystal components in the same layer were in relative equilibrium; and 2) that an equilibration pressure of 1 bar is appropriate.

All data (not averages) are shown in Figures 5-8 and 5-9. The temperatures inferred from Fe-Ti oxides range from 600 °C to 1350 °C. The majority of the data are concentrated in the 750-1200 °C range, regardless of the age interval and location (Figure 5-9). The temperatures inferred from pyroxene range from 800 °C to 1350 °C. The Izu-Bonin pyroxene temperatures (ODP Leg 125 Sites 782A, 784A and 786A pyroxene temperatures) are concentrated in the range 900-1350 °C, while the Mariana pyroxene temperatures (DSDP Leg 60 Sites 458 and 459B pyroxene temperatures) are concentrated in the range 900-1150 °C, regardless of the time period. Clearly, there is a significant difference between the Izu-Bonin and the Mariana pyroxene temperature ranges. However, Arculus and Bloomfield (1992) reported the two-pyroxene temperatures from ~1050 °C (homogeneous, 56 wt% SiO₂) to 780 °C (homogeneous, 76 wt% SiO₂) for ODP Leg 125 ash layers. This temperature range is similar to that of the Marianas. The higher pyroxene temperature ranges of ODP Leg 125 ash layers may be due to more single-pyroxene higher

temperatures (sometimes 100-200 °C higher than two-pyroxene temperatures). This problem will be solved by further comparative study of two-pyroxenes within glasses and the isolated crystals and using more accurate geothermometers.

The 119 data of ilmenite-titanomagnetite (Il-Mt) pairs from all ash layers studied show that the fO_2 falls within ~ 0 to +2.5 log₁₀ units of the synthetic fayalite-magnetite-quartz (FMQ) buffer (Figure 5-8), which is within the range characteristic of island arcs (Arculus et al., 1995). Furthermore, the fO_2 -T range can be subdivided into two groups: higher ΔFMQ values with generally > 1.2 units and lower ΔFMQ values with generally < 1.2 units. The higher ΔFMQ values (1.2-2.5) tend to have higher temperatures (800-1300 °C), while the lower ΔFMQ values (0-1.2) tend to have lower temperatures (600-1000 °C). There are no relationship between the fO_2 and time intervals or locations.

5.5 Summary

From analysis of ~ 1035 plagioclase, ~ 870 pyroxene, ~ 480 Fe-Ti oxides, and a few other mineral phases from 186 representative DSDP Leg 60 and ODP Leg 125 ash layers, the following conclusions can be drawn:

1. The crystalline phases associated with the Izu-Bonin and Mariana glass shards are very similar - predominantly plagioclase, clinopyroxene, orthopyroxene and titanomagnetite with less olivine and ilmenite. Other minerals such as garnet, amphibole, K-feldspar, titanite and apatite are very rare, found only in one to three shards in DSDP Leg 60 Sites 458 and 459B. The lack of amphibole (of similar density to pyroxene) is significant, and indicates perhaps lack of stability of this phase generally in the IBM magma system at low pressures.
2. No systematic differences in plagioclase, pyroxene, or Fe-Ti oxide compositions between the Izu-Bonin and Mariana arcs can be detected. There are no temporal changes for these mineral compositions during at least 35 Ma of eruptive history.

3. There are Mg-rich pyroxene and no plagioclase in three near- basement boninitic ash layers in Site 458. They are boninitic series layers. This Mg-rich pyroxene is completely different from all other pyroxene in the ash layers.

4. The temperatures inferred from pyroxene and Fe-Ti oxides from the Izu-Bonin and Mariana ash layers are concentrated in the range 900-1150 °C and 750-1200 °C, respectively. These are generally within the range of island arcs (Gill, 1981). The temperatures estimated from single-pyroxene thermometry are usually 100-200°C higher than those from two-pyroxene thermometers. Relatively sparse occurrences of assumed coexisting ilmenite-titanomagnetite pairs from the Izu-Bonin and Mariana ash layers define fO_2 's = ~ FMQ + 2.5 log₁₀units, which falls within the range characteristic of island arcs (Arculus et al., 1995).

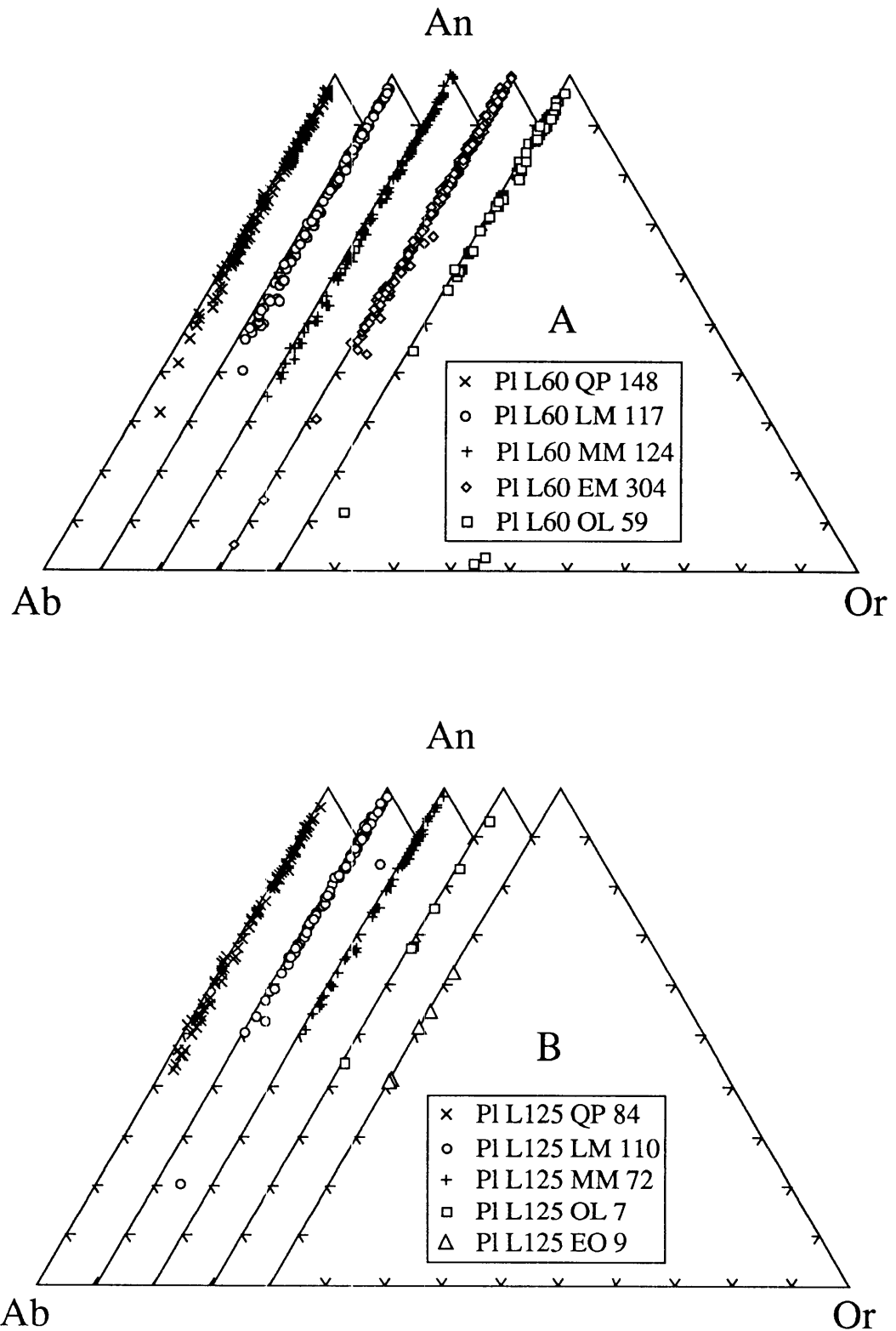


Figure 5-1 Comparison of compositions of plagioclase within DSDP Leg 60 (A) and ODP Leg 125 (B) ash layers. Notation by the specific sample symbols is mineral name followed by leg number, age periods (QP-Quaternary-Pliocene; LM-Late Miocene; MM-Middle Miocene; EM-Early Miocene; OL-Oligocene; and EO-Eocene) and analysis number of individual points. The geologic time scale cited is from the Geological Society of America compiled by Palmer (1983).

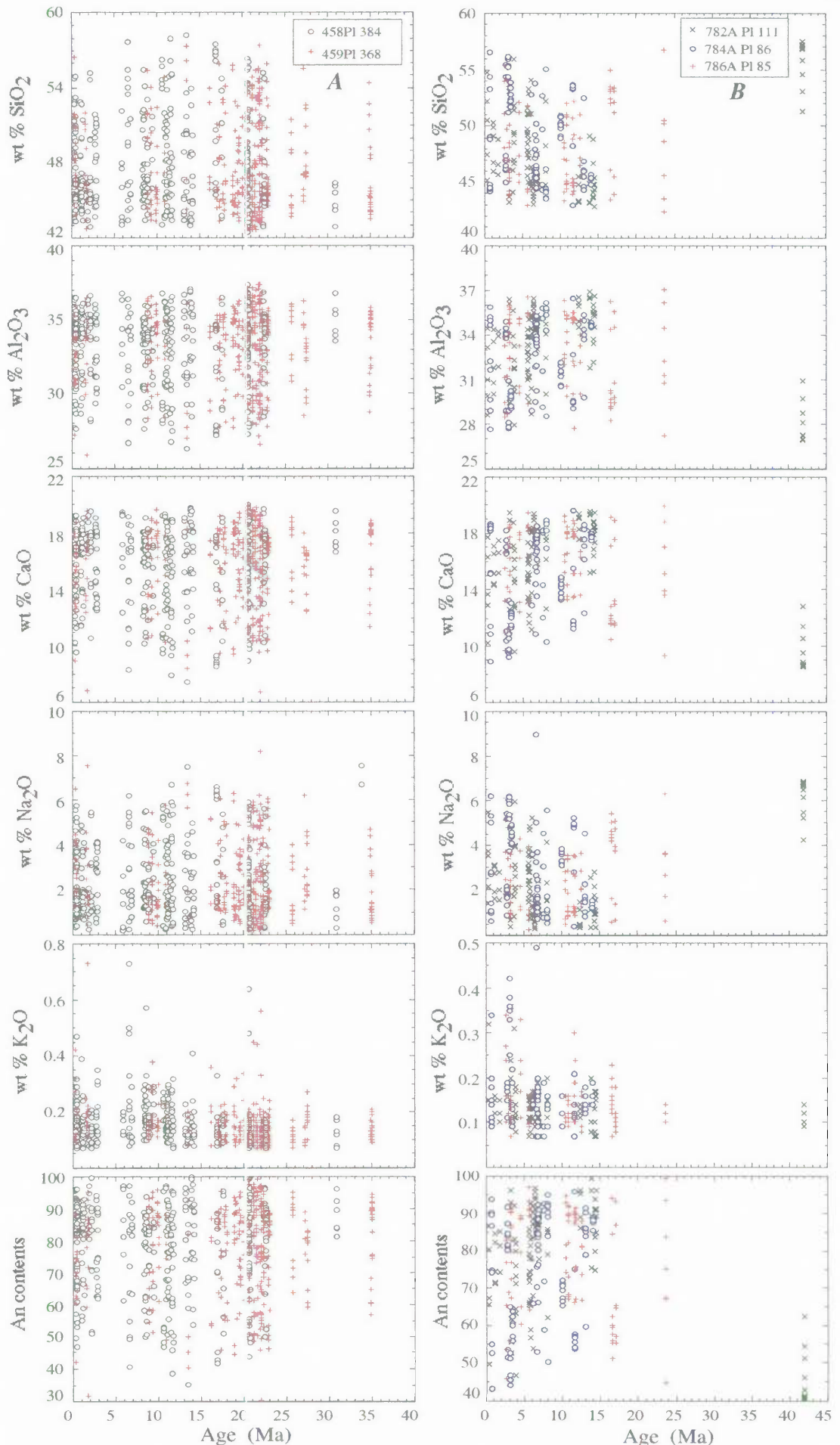


Figure 5-2 Comparison of compositions of plagioclase vs age for DSDP Leg 60 (A) and ODP Leg 125 (B) ash layers. See text and Figure 5-1 for samples.

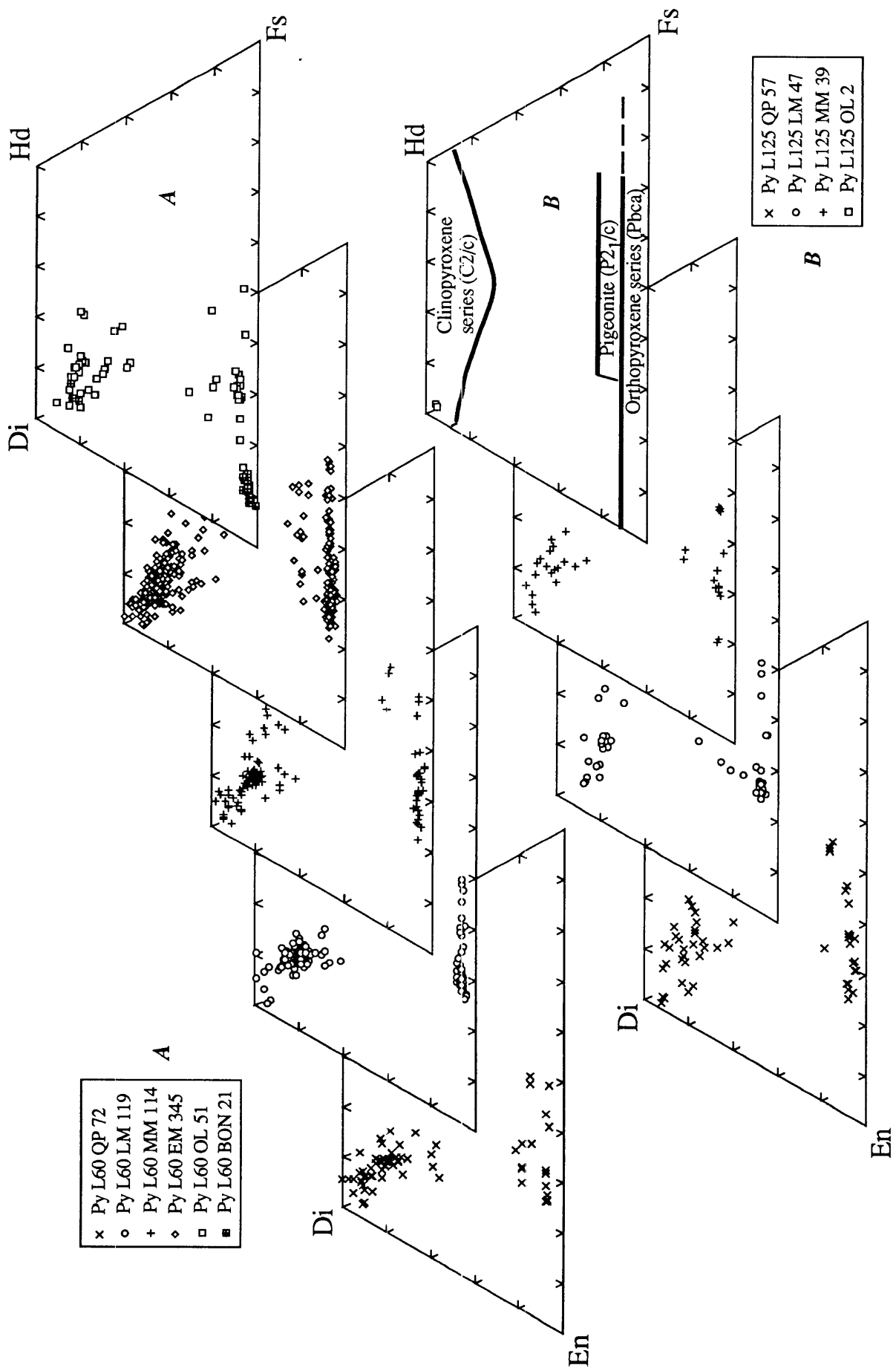


Figure 5-3 Comparison of compositions of pyroxene from DSDP Leg 60 (A) and ODP Leg 125 (B) ash layers. See Figure 5-1 for notation of sample symbols. Additionally, BON is used as boninite abbreviation. The classification lines of Cpc and Opx series and pigeonite are from Klein and Hurlbut (1993).

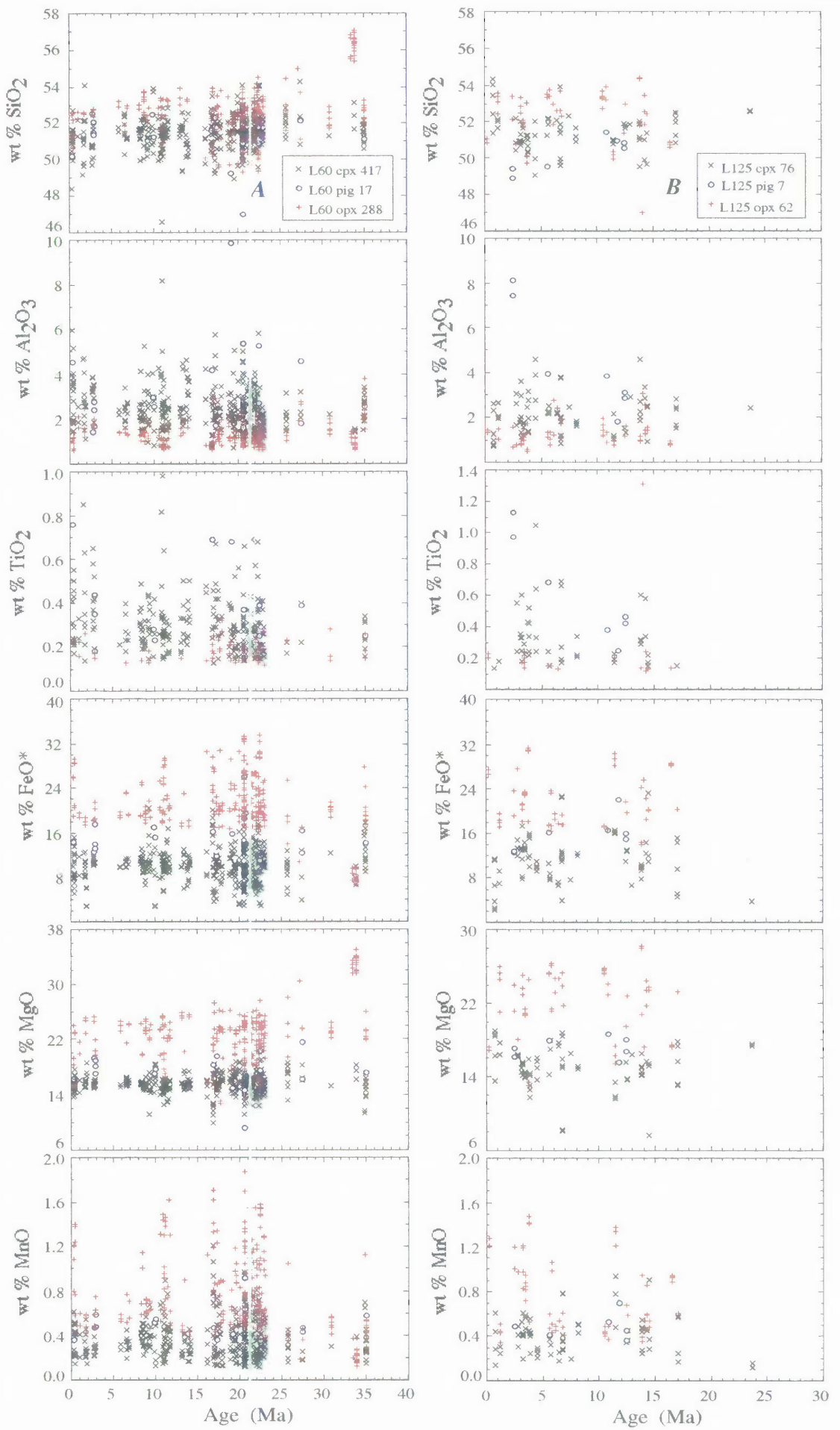


Figure 5-4 Comparison of compositions of pyroxene vs age for DSDP Leg 60 (A) and ODP Leg 125 (B) ash layers. See text and Figure 5-1 for samples.

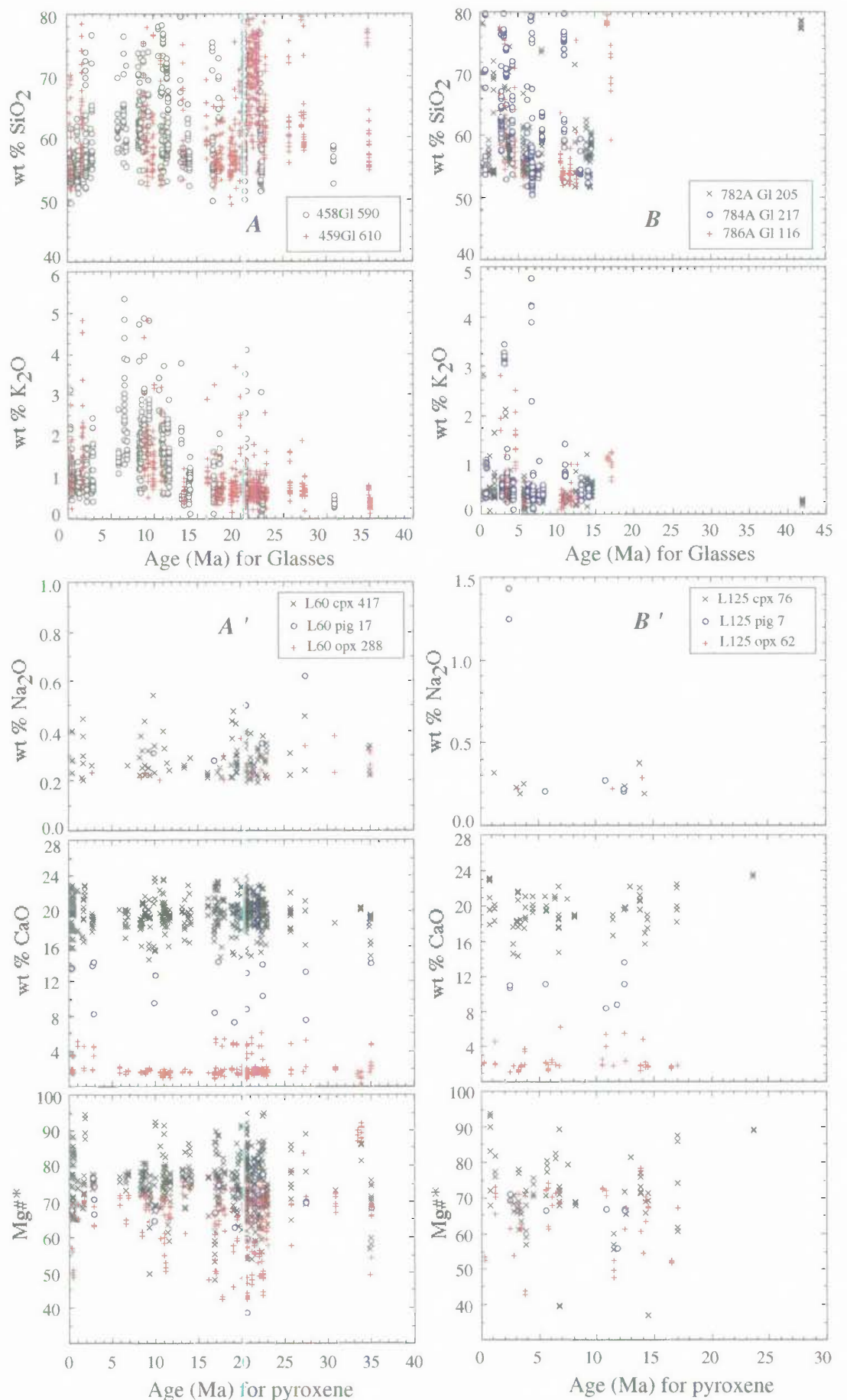


Figure 5-5 Comparison of compositions of glasses vs. age (A and B) and pyroxene vs. age (A' and B') within DSDP Leg 60 and ODP Leg 125 ash layers. See text and Figure 5-1 for samples.

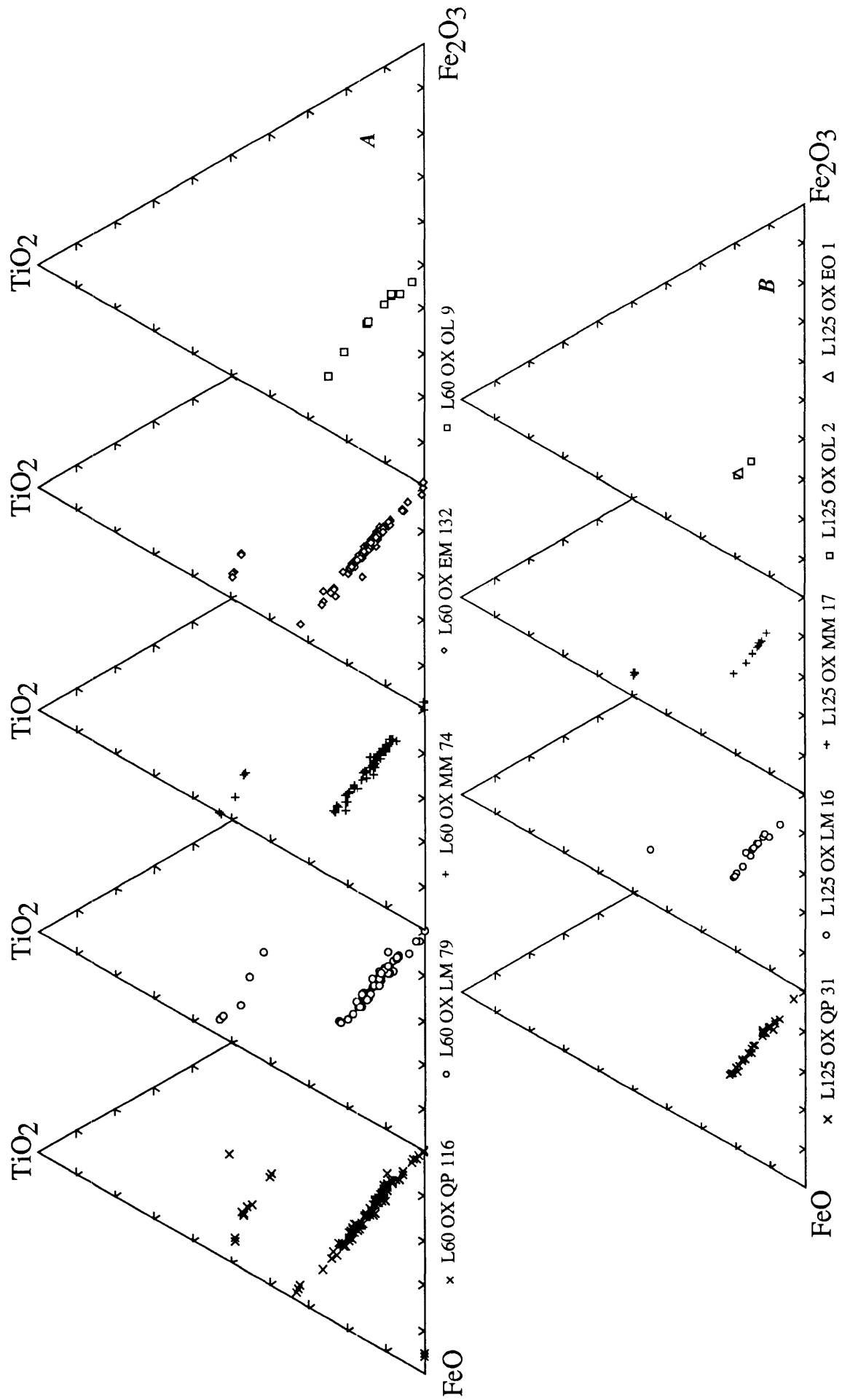


Figure 5-6 Comparison of compositions of Fe-Ti oxides from DSDP Leg 60 (A) and ODP Leg 125 (B) ash layers. See Figure 5-1 for notation of sample symbols.

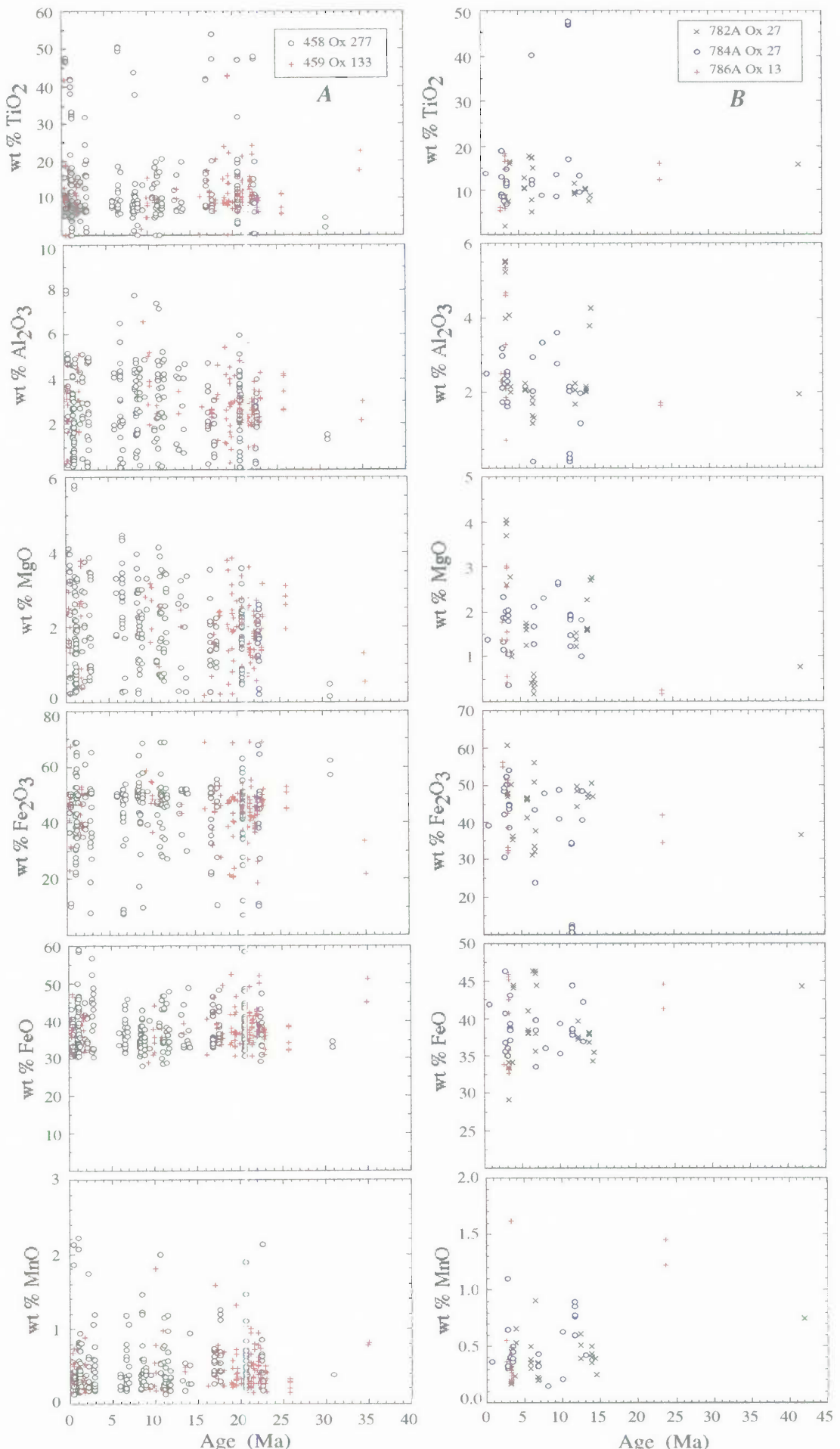


Figure 5-7 Comparison of compositions of Fe-Ti oxides vs age within DSDP Leg 60 (A) and ODP Leg 125 (B) ash layers. See text and Figure 5-1 for samples.

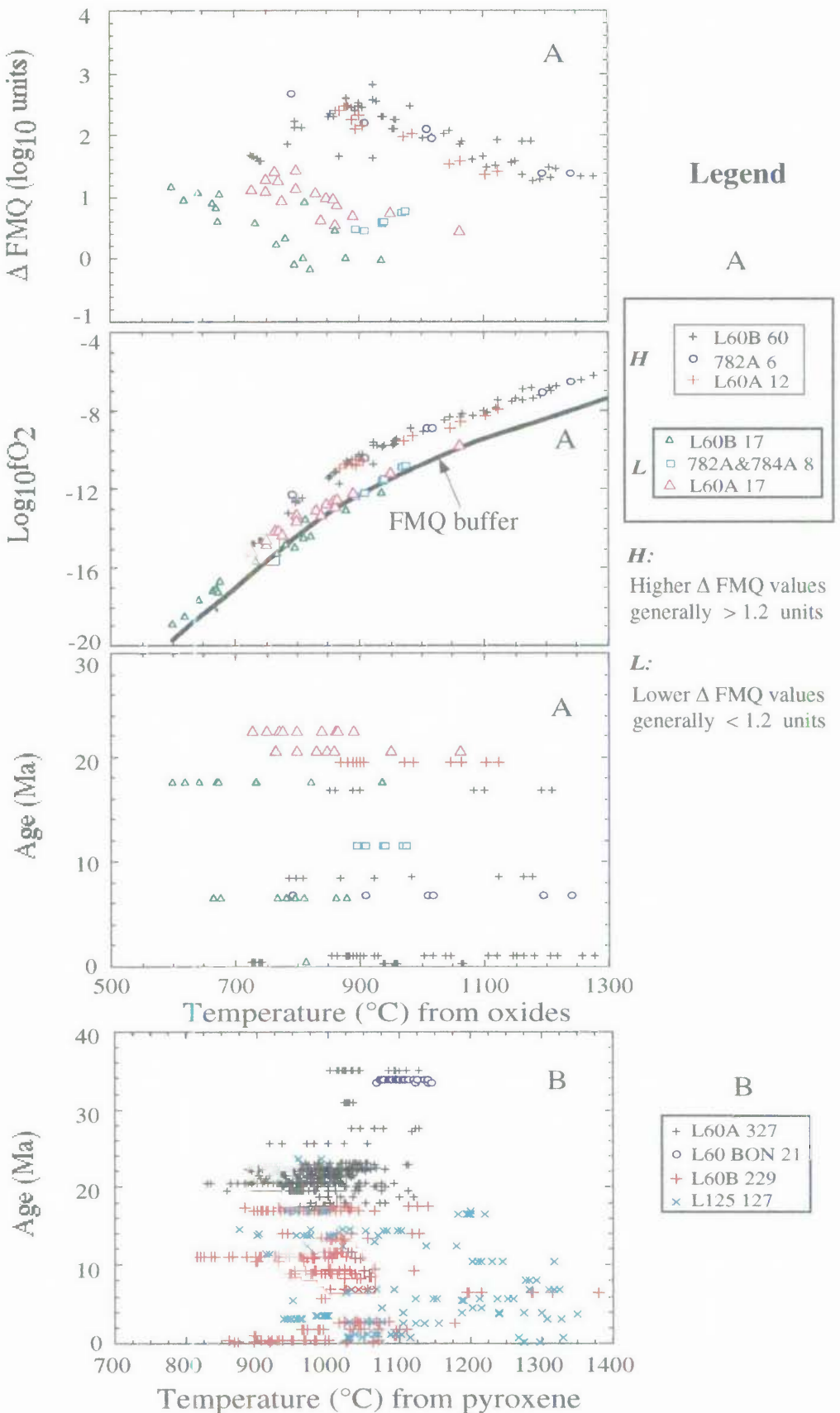


Figure 5-8 Comparison of temperatures inferred from Fe-Ti oxides (A) and pyroxene (B) within DSDP Leg 60 and ODP Leg 125 ash layers. L60A is a time period 0 ~ 17 Ma of DSDP Leg 60 (Sites 458 and 459B) ash layers; L60B, a time period 18 ~ 35 Ma; L60 BON, boninites derived from Site 458 near-basement ash layers. See text for samples and discussion.

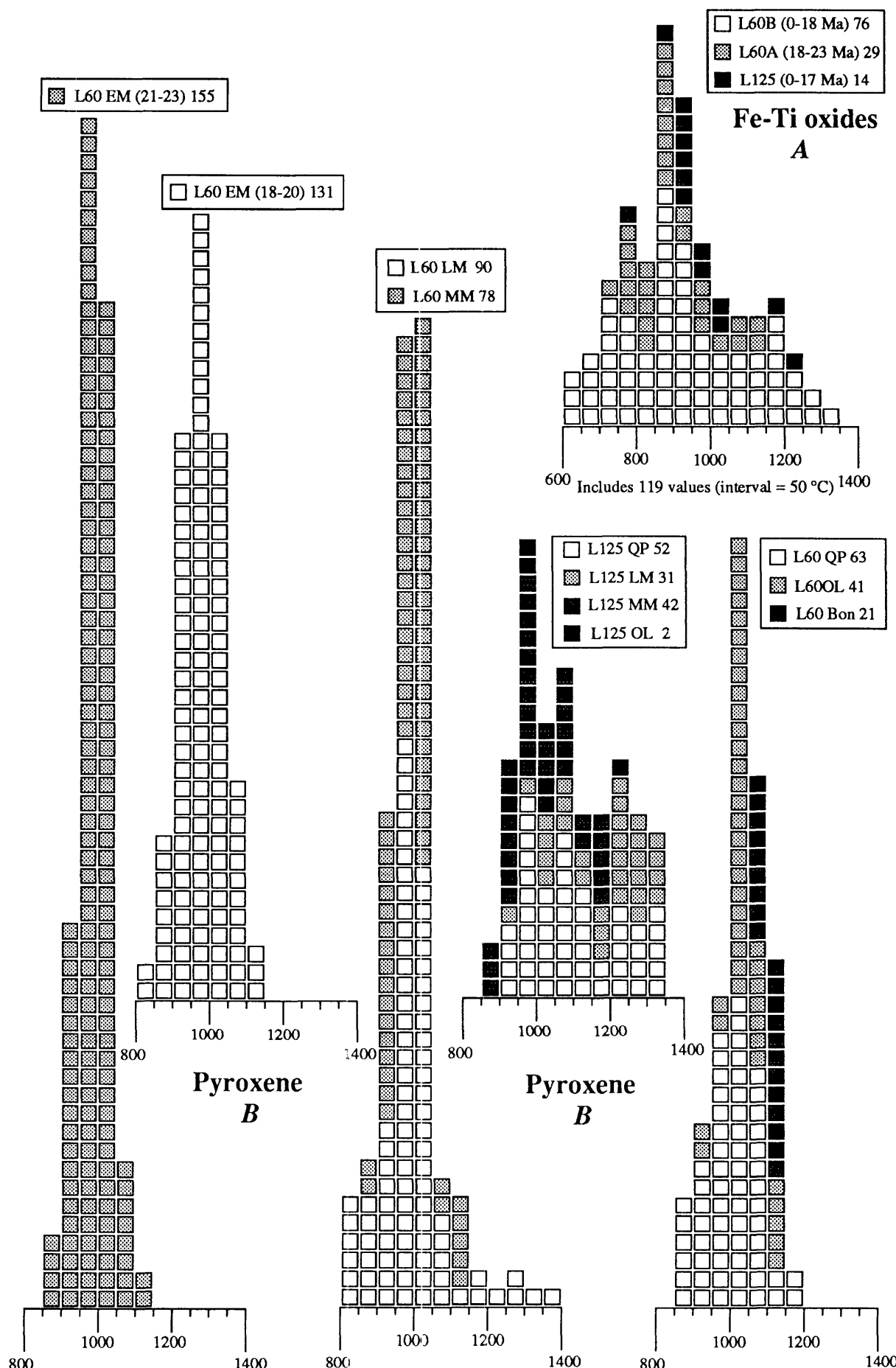


Figure 5-9 Comparison of histograms of temperatures inferred from Fe-Ti oxides (A) and pyroxene (B) from DSDP Leg 60 and ODP Leg 125 ash layers. See Figure 5-1 and 5-8 for legends; see text for discussion.